DOI: 10.1002/ejic.200800420

Synthesis and Characterisation of Two New Iron(II) Spin-Crossover Complexes with N_4O_2 Coordination Spheres – Optimizing Preconditions for Cooperative Interactions

Birgit Weber,*[a] Eike S. Kaps,[a] Cedric Desplanches,[b] Jean-François Létard,*[b] Klaus Achterhold,[c] and Fritz G. Parak[c]

Keywords: Iron / N,O ligands / Magnetism

Two new spin-crossover complexes, $[FeL1(phpy)_2]$ (**1**) and $[FeL2(phpy)_2](phpy)$ (**2**), with L1 and L2 being tetradentate $N_2O_2^{2-}$-coordinating Schiff-base-like ligands {L1 = (*E*,*E*)-[diethyl 2,2′-[1,2-phenylenebis(iminomethylidyne)]bis(3-oxobutanoato)(2–)-*N*,*N*′,O^3,O$^{3\prime}$], L2 = [(3,3′)-[1,2-phenylenebis(iminomethylidyne)]bis(2,4-pentanedionato)(2–)-*N*,*N*′,O^2,O$^{2\prime}$] and phpy = 4-phenylpyridine} have been investigated using temperature-dependent susceptibility and photomagnetic measurements, as well as Mössbauer spectroscopy and X-ray structure analysis. Compound **1** shows a cooperative spin transition with a thermal hysteresis loop approximately 4 K wide ($T_{1/2\downarrow}$ = 232 K and $T_{1/2\uparrow}$ = 236 K). The spin transition of **2** is gradual with $T_{1/2} \approx 290$ K. Results from X-ray structure analysis indicate that the cooperative interactions are due to elastic interactions with several intense C–C contacts in the case of **1**. The change of the spin state at the iron centre is accompanied by a change of the O–Fe–O angle, the so-called bite of the equatorial ligand, from 107° in the high-spin state to 89° in the low-spin state. Reflectivity measurements of **1** indicate that the Light-Induced Excited Spin State Trapping (LIESST) effect occurs at the sample surface at low temperatures. In the bulk solid, photomagnetic properties with a photoexcitation level of 30 % and a *T*(LIESST) value of 41 K are observed using a SQUID magnetometer.

1. Introduction

Spin-transition complexes (spin crossover, SCO) are an interesting class of compounds that can be switched at the molecular level between two or more states by the use of temperature, pressure or light.[1] The bistability of SCO systems is promising for new electronic devices in molecular memories and switches as it may be controlled by different physical perturbations.[2] Octahedral iron(II) complexes with diamagnetic low-spin (LS) and paramagnetic high-spin (HS) states are by far the most thoroughly investigated spin-crossover complexes. However, about 90% of the investigated complexes exhibit an N_6 coordination sphere,[1] while other examples with N_4O_2,[3] N_4S_2,[4] N_4C_2[5] or $N_3C_2O_2$[6] coordination spheres are rare. As part of a more general program, we investigate the properties of mononuclear iron(II) complexes with equatorial Schiff-base-like ligands as possible building blocks for larger systems. Complexes of this ligand type with pyridine,[7,8] 4-(dimethylamino)pyridine[8] or 4-cyanopyridine[9] as axial ligands have already demonstrated that this ligand system is suitable for the synthesis of N_4O_2-coordinated SCO complexes. Different types of spin transitions observed so far (gradual, abrupt, with hysteresis, step-wise) could be correlated with the crystal packing and the extent of short intermolecular contacts. Closer inspection revealed that not only are the number and intensity of short van der Waals contacts significant for the introduction of cooperative effects, but the connection between the contact group and the iron centre is also important. Close contacts between flexible alkyl substituents did not increase the cooperative interactions during the spin transition.[8] Of the different means of transmitting cooperative interactions during a spin transition in mononuclear complexes (hydrogen bonds, π stacking, van der Waals interactions), so far only van der Waals interactions were observed for our class of compounds. In this work we present two new mononuclear spin-crossover complexes with N_4O_2 coordination spheres that use 4-phenylpyridine (phpy) as the axial ligand. The more sterically demanding rigid 4-phenylpyridine might be suitable for introducing a network of π stacking interactions in order to increase the cooperative interactions between the metal centres. Alternatively,

[a] Ludwig-Maximilians-Universität München, Department of Chemistry and Biochemistry,
Butenandtstr. 5–13 (Haus F), 81377 München, Germany
[b] ICMCB, CNRS UPR No 9048 – Université Bordeaux 1, Groupe des Sciences Moléculaires,
87 Av. du Doc. A. Schweitzer, 33608 Pessac, France
[c] Technische Universität München, Physik-Department E17, James-Franck-Strasse, 85747 Garching, Germany
E-mail: bwmch@cup.uni-muenchen.de,
Fax: +49-89-218077407
Supporting information for this article is available on the WWW under http://www.eurjic.org or from the author.

the extent of short van der Waals contacts between rigid ligands could be increased and the spin transition properties could thus be optimised.

2. Results

Scheme 1 gives a schematic representation of the ligands used in this work. H_2L1 and H_2L2 were synthesised as described in the literature,[10] and their reaction with iron(II) acetate in methanol in the presence of 4-phenylpyridine (phpy) gave compounds **1** [FeL1(phpy)$_2$] and **2** [FeL2(phpy)$_2$](phpy) in good yields. The complexes were fully characterised by elemental analysis, IR and mass spectroscopy as well as X-ray diffraction at different temperatures. The magnetic properties were determined by *T*-dependent susceptibility measurements using a SQUID magnetometer at two different field strengths (2000 and 5000 G) and Mössbauer spectroscopy.

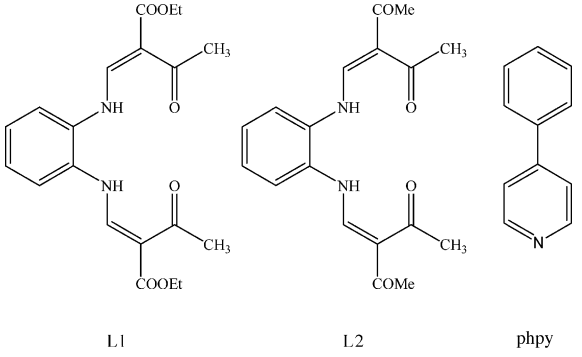

Scheme 1. Schematic representation of the ligands used in this work.

2.1. Magnetic Properties

Figure 1 gives the temperature dependence of the magnetic properties of **1** and **2** (plot of the $\chi_M T$ product vs. *T*) analysed in the 5–350 K temperature range. The room-temperature value of $\chi_M T$ for **1** is 3.17 cm^3 K mol^{-1}, which is within the region expected for a HS iron(II) centre. Upon cooling the moment remains constant until about 250 K where an abrupt transition into the LS state takes place. A 4 K-wide thermal hysteresis loop is observed with a characteristic temperature (estimated for a HS molar fraction, γ_{HS}, of 0.5) of $T_{1/2\downarrow}$ = 232 K and $T_{1/2\uparrow}$ = 236 K. In the low-temperature region all iron centres are essentially in the LS state with $\chi_M T$ = 0.09 cm^3 K mol^{-1}. The room temperature value of $\chi_M T$ for **2** is 1.75 cm^3 K mol^{-1}, which is significantly smaller than the value expected for HS iron(II). Upon heating the moment increases until it reaches a value of 2.78 cm^3 K mol^{-1} at 350 K. The compound is still not completely in the HS state. The temperature was not increased further as the sample decomposes at higher temperatures. Upon cooling a gradual transition into the LS state is observed that is complete at approximately 200 K. The $T_{1/2}$ value is in the region of 290 K. The low-temperature value of $\chi_M T$ at 150 K is 0.01 cm^3 K mol^{-1}, all iron centres are essentially in the LS state.

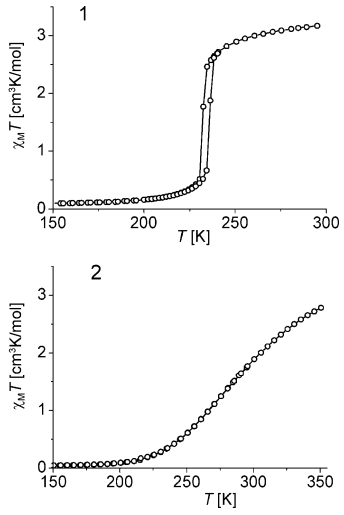

Figure 1. Plot of the $\chi_M T$ product vs. *T* for compounds **1** and **2**.

For a better comparison, the intermolecular interaction parameter, *Γ*, was determined using the mean-field model proposed by Schlichter and Drickamer [Equation (1)][11].

$$\Delta G_{HL} = \Delta H_{HL} - T\Delta S_{HL} + \Gamma(1 - 2\gamma_{HS}) \quad (1)$$

where ΔG_{HL}, ΔH_{HL} and ΔS_{HL} are the free energy, enthalpy and entropy changes, respectively, associated with the spin transition. This was done by least-squares fittings of the γ_{HS} vs. *T* curves of the two complexes. The obtained fitting parameters are ΔH_{HL} = 15.3 ± 0.7 kJ mol^{-1}, ΔS_{HL} = 65.6 ± 2.8 J mol^{-1} K^{-1} and Γ = 4.0 ± 0.1 kJ mol^{-1} for **1** and ΔH_{HL} = 18.0 ± 0.6 kJ mol^{-1} and ΔS_{HL} = 62.3 ± 2.3 J mol^{-1} K^{-1} for **2**. In Figure S1 of the Supporting Information, the fit of γ_{HS} vs. *T* is represented for the two complexes with the used parameters indicated. Following the suggestion of Purcell et al.[12] the parameter *C* (= $\Gamma/2RT_{1/2}$ = cooperativity factor) was determined. Its value is 1.03 for compound **1**. This is in good agreement with the small thermal hysteresis observed. For compound **2** no cooperative interactions are observed and the value of *C* is therefore zero.

The spin transition of **1** was also followed using Mössbauer spectroscopy between 265 K and 200 K in heating and cooling modes. Selected spectra at different temperatures are given in Figure 2 with the high-spin mole fraction indicated. Values of the Mössbauer parameters obtained by least-squares fitting of the spectra are gathered in Table S1 of the Supporting Information. At 265 K the Mössbauer spectrum consists of a unique quadrupole-split doublet, with an isomer shift, δ, of 1.09 mm s^{-1} and a quadrupole splitting, ΔE_Q, of 2.55 mm s^{-1}. These parameters are typical for HS iron(II). Below 250 K a LS iron(II) doublet appears with the parameters δ = 0.47 mm s^{-1} and ΔE_Q = 1.39 mm s^{-1} at 200 K. The high-spin mole fraction at each temperature was deduced from the area ratio, A_{HS}/A_{tot} (A_{HS} = area of the HS doublet, A_{tot} = total Mössbauer absorption), deter-

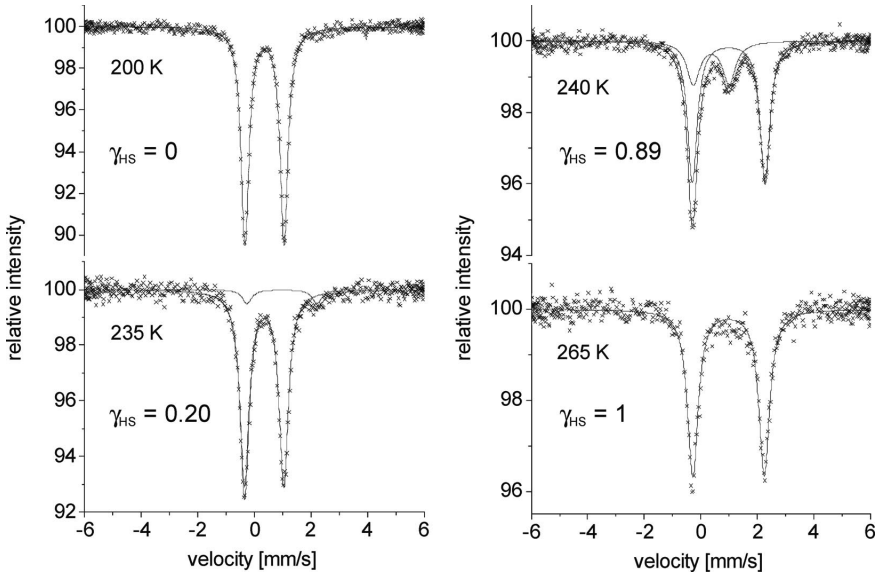

Figure 2. Plot of the Mössbauer spectra of compound **1** at 200, 235, 240 and 265 K with the high-spin molar fraction indicated.

mined from the least-squares fitting of the spectra and corrected by the Lamb Mössbauer factor. All further details are given in the Supporting Information. The transition temperature, $T_{1/2\uparrow}$, of 237 K is in good agreement with the results from susceptibility measurements. Because of the high transition temperature of **2** no Mössbauer spectra were collected for this compound.

2.2. X-ray Structure Analysis

Crystals suitable for X-ray structure analysis have been obtained for both complexes. Selected bond lengths and angles within the first coordination sphere are summarised in Table 1. Ortep representations of the LS forms of **1** and **2** are given in Figure 3 and Figure 4. In the case of **1**, the X-ray structure was measured before and after the spin transition. For compound **2** the spin transition is still not complete at room temperature, and the X-ray structure was therefore only determined in the LS state

Intramolecular changes during the spin transition: The average bond lengths of the iron centre in the high-spin state are 2.08 Å (Fe–N_{eq}), 2.01 Å (Fe–O_{eq}) and 2.26 Å (Fe–N_{ax}). Upon spin transition a shortening of the bond lengths by about 10%, as discussed for other iron(II) spin-crossover complexes in the literature, is observed. This shortening is more pronounced for the axial ligands than for the equatorial ones. The average bond lengths in the low-spin state are 1.91 Å (Fe–N_{eq}), 1.96 Å (Fe–O_{eq}) and 2.01 Å (Fe–N_{ax}). A sensible tool for determining the spin state of this type of

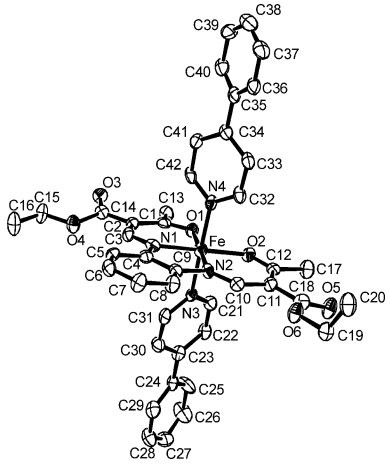

Figure 3. ORTEP representation of the asymmetric unit of **1** at 130 K and atom numbering scheme used for the discussion of the intermolecular distances. Hydrogen atoms were omitted for clarity. Thermal ellipsoids are shown at the 50% probability level.

iron complex is the O–Fe–O angle, the so-called bite of the ligand. It changes from 107° in the high-spin state to an average of 89° in the low-spin state.

Intermolecular interactions: Selected intermolecular distances for **1** and **2** are reported in Tables S2 and S3 of the Supporting Information, respectively. Selected views of the packing of the molecules of **1** and **2** in the crystal are given in Figure 5 and Figure 6, respectively. Compound **2** shows a gradual spin transition with no indications of cooperative

Table 1. Selected bond lengths [Å] and angles [°] within the first coordination sphere of the iron complexes discussed in this work.

Complex	T [K]	S	Fe–N1/2	Fe–O1/2	Fe–N3/4	O1–Fe–O2	N_{ax}–Fe–N_{ax}	∠L1, L2c
1	300	2	2.078(2)/2.081(3)	2.000(2)/2.009(2)	2.229(3)/2.289(3)	107.25(8)	174.47(9)	61.3
1	130	0	1.921(4)/1.922(3)	1.952(3)/1.967(3)	1.989(4)/2.009(3)	89.5(1)	174.7(1)	73.6
2	125	0	1.902(2)/1.910(2)	1.950(2)/1.952(2)	2.013(3)/2.015(3)	89.11(8)	174.84(9)	81.1

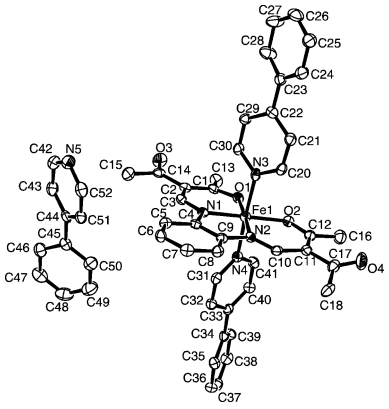

Figure 4. ORTEP representation of the asymmetric unit of **2** at 125 K and atom numbering scheme used for the discussion of the intermolecular distances. Hydrogen atoms were omitted for clarity. Thermal ellipsoids are shown at the 50% probability level.

interactions. This is in agreement with the presence of only a few direct short intermolecular contacts. Some additional contacts mediated by the additional 4-phpy can be observed; however, for the communication of elastic interactions those contacts are of little relevance. In total the packing can be described as a 1D chain of linked molecules. Additionally, it has been demonstrated for a series of mixed crystals of the general composition $[M_{1-x}Fe_x(pic)_3]X_2 \cdot solv$ (solv = MeOH, EtOH; X = Cl, Br; M = Co, Zn, Mn) that the interaction constant decreases with decreasing x until a gradual spin transition is observed.[13] A similar dilution effect is responsible for the gradual spin transition of compound **2** with the difference that, instead of a metal-substituted inert complex molecule, the additional axial ligand molecule is the diluent. In the case of **1**, four different short contacts of the C–H···A type (A = acceptor atom) build a 3D network of linked molecules that is supported by additional H···H and H···C van der Waals contacts. Upon cooling a shortening of all the contacts except one is observed. Those interactions satisfactorily explain the small hysteresis observed in the magnetic measurements.

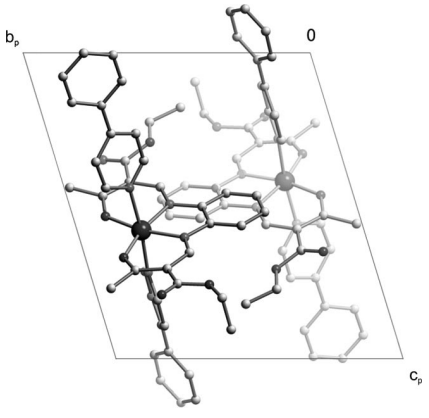

Figure 5. Projection of the packing of the molecules of **1** in the HS state along the *a* axis.

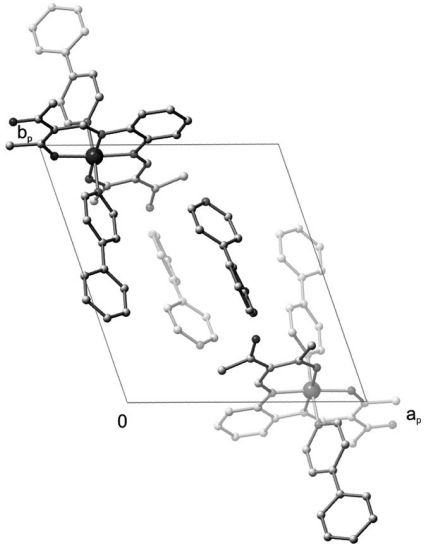

Figure 6. Projection of the packing of the molecules of **2** in the LS state along the *c* axis.

Of the complexes investigated so far the equatorial ligand L1 only leads to gradual SCO materials,[7,9] except for in the $[FeL1(Him)_2]$ complex where a 4 K-wide thermal hysteresis loop is observed that is attributed to a hydrogen bond network.[7c] If only examples with van der Waals contacts are considered, the use of 4-phpy as the axial ligand significantly improved the SCO properties of the system and our synthetic strategy was successful. This is different for the complexes of L2. Here abrupt spin transitions with small hysteresis loops (2 K and 9 K)[8] were reported – the gradual transition of the 4-phpy complex, **2**, is a setback with regard to our synthetic strategy. Now the question arises as to whether it is possible to determine the parameters for the crystal engineering of SCO complexes with cooperative interactions due to short van der Waals contacts, or more specifically, how can a maximum number of relevant contacts be obtained? This question might be of great importance for the future design of highly cooperative spin-crossover complexes, especially since we recently demonstrated with a 4,4′-bipyridine-bridged complex that covalent linkers are probably not useful for transmitting cooperative interactions.[14,15] This implicates that the importance of noncovalent interactions increases again, and the question of how the spreading of those contacts through the crystal can be controlled gains importance.

One aspect that could be optimized and which is under the control of a preparative chemist is the shape of the molecule. Homoleptic SCO complexes can easily be idealized as spheres, and a dense spherical packing can be easily imagined. This is not the case for our compounds, whose shape could instead be described as ellipsoidal. Therefore we measured the three diameters, *a*, *b* and *c*, defined according to Scheme 2, to obtain some parameters describing the shape of the molecule that can be controlled. The results are summarised in Table 2. Two simple rules can be defined by comparison of the data for six available complexes: (a) the diameter length ordering $a \geq b > c$ appears to be a

good one for the design of cooperative complexes (this describes an ellipsoid slightly prolated in the direction of the axial ligand), and (b) the ellipsoid obtained should not be too prolated (e.g., the rule $|a - b| \cong |b - c|$ could see to this). This implicates that small changes in the substituents of the ligands (e.g., a methyl instead of an ethyl group in L1) can drastically improve the SCO properties of the compound, and we will start preparing new mononuclear complexes bearing these considerations in mind to see if the idea works.

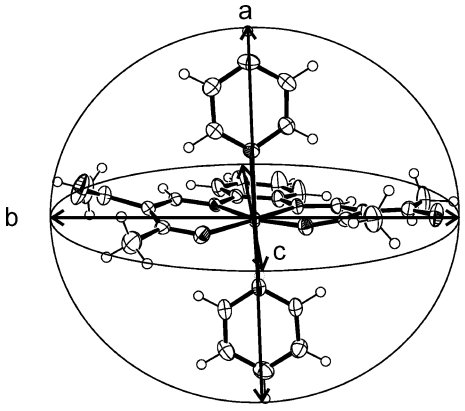

Scheme 2. Schematic representation of the octahedral complex with the diameters summarised in Table 2.

Table 2. Diameters [Å] of octahedral iron(II) complexes of the Schiff-base-like N_2O_2-coordinating ligands discussed in this work.

Compound	$T_{1/2}$ [K]	C	HS			LS			Ref.
			a	b	c	a	b	c	
[FeL1(py)$_2$]	220	0	11.9	16.2	9.1	11.6	16.0	9.1	[7b]
[FeL1(CNpy)$_2$]	238	≈ 1	15.1	16.8	9.1	14.7	16.6	9.2	[9]
1	234	1.03	20.5	16.1	9.0	20.1	16.3	9.3	this work
[FeL2(py)$_2$]	190	1.08	11.9	12.9	9.1	11.5	12.8	9.2	[8]
[FeL2(dmap)$_2$]	179	1.28	16.1	12.9	9.1		/		[8]
2	290	0		/		20.1	12.8	9.2	this work

2.3 Optical and Photomagnetic Measurements

For the two complexes the thermal spin-crossover behaviour has been followed by measuring the diffuse absorption spectra (Figure 7). When the temperature is cooled from room temperature to 150 K the absorption band at around 850 nm, characteristic of the d–d transition of the HS state, decreases. In the visible range that is linked to the LS state (MLCT and d–d transitions), only a slight increase is recorded upon cooling. This is due to the near saturation of the spectra, which is in agreement with the dark colour of the compounds observed at room temperature. Figure 8 reports an alternative way to follow the change in the diffuse absorption spectra as a function of temperature by measuring the change of the reflectivity spectra at selected wavelengths, i.e. 884 and 850 nm (compounds **1** and **2** respectively). With the thermal HS → LS spin transition the intensity of the transition band at 884 nm/850 nm decreases, and the reflectivity signal consequently increases. But what is interesting to note is that for temperatures below 50 K, the reflectivity signal of **1** decreases. This is in agreement with the diffuse absorption spectra, which recover the shape and intensity they had at 250 K. These observations provide some evidence that i) at the surface the light-induced LS → HS conversion occurs, according to the LIESST phenomenon,[16] and ii) the lifetime of the photoinduced HS state below 50 K is sufficiently long to allow optical excitation by a halogen light source delivering around 5 mW cm^{-2}. In contrast to this, no indication for a light-induced LS → HS conversion is observed for compound **2**. This is in agreement with the inverse energy gap law introduced by Hauser[17] or the T(LIESST) vs. $T_{1/2}$ relation of Létard.[18,19] According to both, higher $T_{1/2}$ values result in a destabilisation of the photoinduced HS state as observed

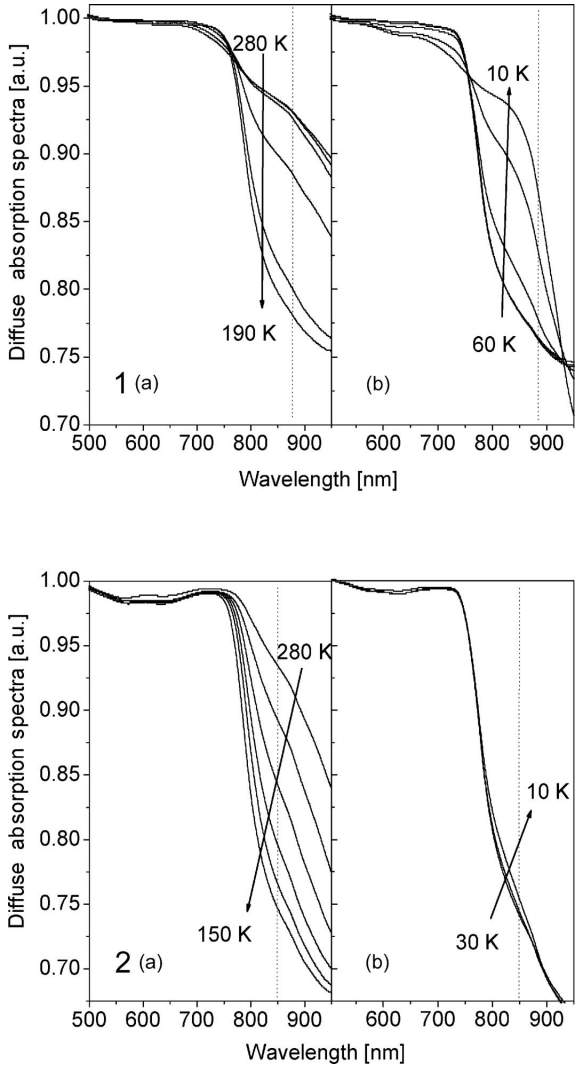

Figure 7. Diffuse absorption spectra of **1** and **2** as a function of both temperature and light irradiation with (a) the thermal spin crossover and (b) the light-induced regions.

when going from compound **1** to **2**. As a consequence we have decided to only perform the photomagnetic investigation (i.e., in the bulk solid) on sample **1**.

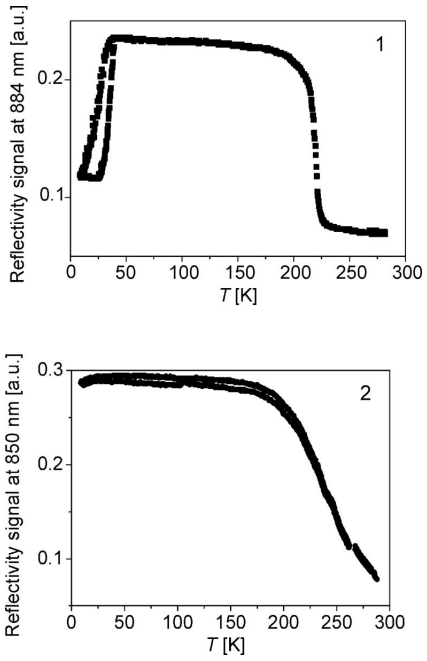

Figure 8. Reflectivity signal of **1** and **2** at a selected wavelength as a function of both temperature and light irradiation.

The irradiation experiment was performed by using a laser emitting red light between 647.1 and 676.4 nm. About 30% of the molecules could be excited into the photoinduced high-spin state. The plot of the T(LIESST) experiment is reported in Figure 9. In this procedure, the irradiation was maintained until complete saturation of the signal was obtained, then the light was switched off and the temperature slightly increased at 0.3 K min^{-1}. The minimum of the d$\chi_M T$/dT vs. T curve defines the T(LIESST) limit temperature (i.e., 41 K for **1**), above which the light-induced magnetic HS information is erased in the SQUID cavity.[20]

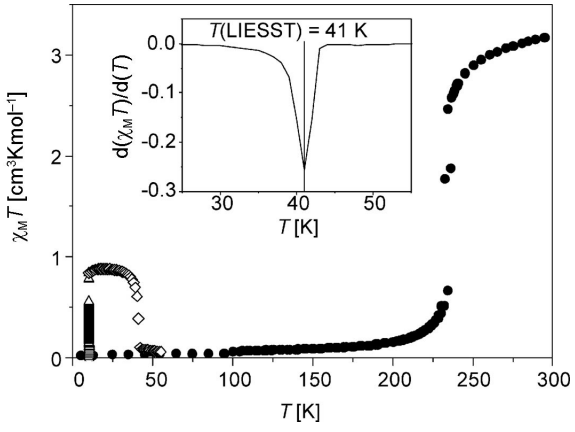

Figure 9. Temperature dependence of $\chi_M T$ for **1**. • = data recorded in the cooling and warming modes without irradiation; Δ = data recorded with irradiation at 10 K at 674.1–676.4 nm; ✧ = T(LIESST) measurement: data recorded in the warming mode with the laser turned off after irradiation for one hour.

The low level of photoexcitation is in agreement with the dark colour of **1** observed. This has some strong consequences for quantitatively inducing light excitation in the bulk solid. If the opacity of the sample is significant, the penetration of light can be inhibited and the photoexcitation appears incomplete. The sample can be described as having two phases: a top phase at the surface saturated in terms of photoexcitation and a bottom phase practically unexcited. Because of the low level of photoexcitation, no further kinetic studies were performed.

3. Concluding Remarks

In this work we have described the synthesis and characterisation of two new SCO complexes. Results from X-ray structure analysis indicate that the 4 K-wide hysteresis loop in the case of **1** is due to several close intermolecular contacts, as observed for similar complexes with this type of ligand. In the case of compound **2** a gradual transition is observed that can be explained by the additional 4-phenylpyridine molecule in the crystals. Attempts were made to better understand and predict the packing of the molecules in the crystal by comparing six SCO complexes of this ligand type with different types of spin-transition behaviour.

Because of the dark colour of the compound, the measured reflectivity spectra were close to saturation. However, some indication of LIESST properties was detected for compound **1**. Of course, the level of photoexcitation in the bulk solid was only about 30%; the LS → HS photoconversion process was more evident at the surface. With a T(LIESST) of about 41 K for compound **1**, the stabilization of the photo-induced HS state appears to be very weak. This work confirms a recent study performed on other spin-crossover complexes belonging to a similar family[8,9] that involve this type of tetradentate ligand which possesses a degree of flexibility around the unsaturated nitrogen atoms connecting the aromatic phenyl rings, and it emphasizes the concept that vibrational aspects and the hardness of the inner coordination sphere are the key factors for stabilizing the metastability of the light-induced HS state.[18a,19c]

Experimental Section

Syntheses: All syntheses were carried out under argon using Schlenk techniques. Methanol was purified as described in the literature[20] and distilled under argon. The synthesis of H_2L1,[10] H_2L2[10] and iron(II) acetate[21] is described in the literature. Phpy is commercially available and was used without further purification.

[FeL1(phpy)$_2$] (1): H_2L1 (0.79 g, 2.03 mmol), iron(II) acetate (0.46 g, 2.64 mmol) and phpy (4.73 g, 0.030 mol) were dissolved in methanol (30 mL) and heated at reflux for 2 h. After cooling, a fine black crystalline precipitate was obtained that was filtered off, washed with methanol (10 mL) and dried in vacuo. Yield 0.91 g (59%). $C_{42}H_{40}FeN_4O_6$ (752.6): calcd. C 67.02, H 5.36, N 7.44; found C 67.32, H 5.33, N 7.45. IR (Nujol): $\tilde{\nu}_{C=O}$ = 1688 cm^{-1}. MS (DE): m/z (%) = 155 (100) [phpy]$^+$, 442 (65) [M]$^+$.

[FeL2(phpy)$_2$](phpy) (2): H_2L2 (0.88 g, 2.67 mmol), iron(II)acetate (0.61 g, 3.51 mmol) and phpy (6.27 g, 0.040 mol) were dissolved in

methanol (30 mL) and heated at reflux for 2 h. After cooling, a fine black crystalline precipitate was obtained that was filtered off, washed with methanol (10 mL) and dried in vacuo. Yield 1.63 g (71%). $C_{51}H_{45}FeN_5O_4$ (847.8): calcd. C 72.25, H 5.35, N 8.26; found C 72.65, H 5.41, N 8.25. IR (Nujol): $\tilde{\nu}_{C=O}$ = 1636 cm^{-1}. MS (DEI): *m/z* (%) = 155 (100) $[phpy]^+$, 382 (25) $[M]^+$.

Physical Measurements: Magnetic measurements of pulverised samples were performed on a Quantum Design MPMSR-XL SQUID magnetometer over a 2–350 K temperature range. All measurements were carried out at two field strengths (0.2 and 0.5 T) in the settle mode. The data were corrected for the magnetisation of the sample holder, and diamagnetic corrections were estimated using Pascal's constants. Elemental analysis was performed on an Elementar Vario EL instrument.

Mössbauer spectra were recorded using a conventional Mössbauer spectrometer operating in a sinusoidal velocity profile. The sample was placed in a bath cryostat (Cryo Industries of America Inc., Modell 11CC).

For the LIESST measurements, the measurement of the diffuse absorption spectra and reflectivity signal were performed by using a custom-built setup equipped with a SM240 spectrometer (Opton Laser International). This equipment allowed us to record both the diffuse absorption spectra within the 500–900 nm range at a given temperature and the temperature dependence (5–290 K) of the reflectivity signal at a selected wavelength (± 2.5 nm). The diffuse reflectance spectrum was calibrated with respect to activated charcoal (Merck) as a black standard and barium sulfate ($BaSO_4$, Din 5033, Merck) as a white standard.

The photomagnetic measurements were performed using a Spectra Physics Series 2025 Kr^+ laser (647.1–676.4 nm) coupled through an optical fibre to the cavity of the MPMS-55 Quantum Design SQUID magnetometer operating with an external magnetic field of 2 T within a 2–300 K temperature range and at a speed of 10 K min^{-1} in the settle mode at atmospheric pressure.[18,19] The power of the laser beam on the sample for the selected wavelength(s) used was adjusted to 5 mW cm^{-2}. The bulk attenuation of light intensity was limited as much as possible by the preparation of a thin layer of compound. It is noteworthy that there was no change in the data resulting from sample heating upon laser irradiation. The weight of these thin-layer samples (approximately 0.2 mg) was obtained by comparison of the measured thermal spin-crossover curve with another curve of a more accurately weighed sample of the same compound. The data were corrected for the magnetisation of the sample holder and for diamagnetic contributions, estimated from Pascal's constants.

Crystal Structure Determinations: The intensity data of **1** and **2** were collected on a Nonius KappaCCD diffractometer using graphite-monochromated Mo-K_α radiation. Data were corrected for Lorentz and polarisation effects and for absorption (XRed).[22] The structures were solved by direct methods (SIR97)[23] and refined by full-matrix least-squares techniques against F_o^2 (SHELXL-97).[24] The hydrogen atoms were included at calculated positions with fixed thermal parameters. All non-hydrogen atoms were refined anisotropically. Cell parameters and refinement results for all complexes are summarized in Table 3. ORTEP-III was used for structure representation.[25]

CCDC-670131 (for **1**, at room temp.), -670132 (for **1**, at 130 K), and -670133 (for **2**, at 125 K) contain the supplementary crystallographic data. These data can be obtained free of charge from The Cambridge Crystallographic Data Centre via www.ccdc.cam.ac.uk/data_request/cif.

Supporting Information (see footnote on the first page of this article)**:** Least-squares fitting results of the thermal variation of γ_{HS} for **1** and **2** (Figure S1), the details for the analysis of the Mössbauer spectra together with the least-squares-fitted Mössbauer data (Table S1 and Figure S2) and selected intermolecular distances for **1** and **2** (Tables S2 and S3).

Table 3. Crystallographic data for octahedral iron(II) complexes discussed in this work.

	[FeL1(phpy)$_2$] (HS)	[FeL1(phpy)$_2$] (LS)	[FeL2(phpy)$_2$](phpy) (LS)
Formula	$C_{42}H_{40}FeN_4O_6$	$C_{42}H_{40}FeN_4O_6$	$C_{51}H_{45}N_5O_4Fe$
MW [g mol^{-1}]	752.635	752.635	847.8
Crystal system	triclinic	triclinic	triclinic
Space group	$P\bar{1}$	$P\bar{1}$	$P\bar{1}$
λ [Å]	0.71073	0.71073	0.71073
T [K]	298(2)	130(2)	125(2)
Crystal size [mm]	0.46 × 0.25 × 0.23	0.47 × 0.27 × 0.23	0.12 × 0.10 × 0.07
a [Å]	11.7640(7)	11.8390(13)	11.8270(8)
b [Å]	12.3600(10)	12.4310(19)	13.4788(11)
c [Å]	13.9680(7)	13.599(2)	14.8644(10)
α [°]	104.997(6)	103.249(15)	104.314(4)
β [°]	102.265(5)	101.906(12)	103.280(4)
γ [°]	96.475(6)	99.711(11)	104.183(4)
V [Å^3]	1886.5(2)	1856.5(5)	2117.1(3)
Z	2	2	2
$d_{calcd.}$ [g cm^{-1}]	1.32499(14)	1.3464(4)	
μ [mm^{-1}]	0.453	0.460	0.409
Absorption correction	numerical	numerical	numerical
Reflections collected	8916	7692	14289
Independent reflections (R_{int})	6646 (0.0474)	5918 (0.0743)	7422 (0.0731)
Data/restraints/parameters	6646/0/483	5918/0/507	7422/0/555
Final R indices [$I > 2\sigma(I)$]	R_1 = 0.0477, wR_2 = 0.0971	R_1 = 0.0631, wR_2 = 0.1357	R_1 = 0.0500, wR_2 = 0.0946
R indices (all data)	R_1 = 0.1086, wR_2 = 0.1155	R_1 = 0.1181, wR_2 = 0.1650	R_1 = 0.1038, wR_2 = 0.1094
Goodness of fit	0.877	0.973	0.953

Acknowledgment

This work has been supported financially by the Deutsche Forschungsgemeinschaft (DFG) (SPP 1137) and the Fonds der Chemischen Industrie. The authors would also like to thank the Aquitaine Region for funding the Photomagnetic platform at the ICMCB, the ANR Fast-switch (NT05-3_45333) and the network of excellence MAGMANet (FP6-515767-2). B. W. would like to thank S. Albrecht for the acquisition of the crystallographic data.

[1] a) H. A. Goodwin, *Coord. Chem. Rev.* **1976**, *18*, 293; b) P. Gütlich, *Struct. Bonding (Berlin)* **1981**, *44*, 83; c) E. König, *Prog. Inorg. Chem.* **1987**, *35*, 527; d) P. Gütlich, A. Hauser, *Coord. Chem. Rev.* **1990**, *97*, 1; e) E. König, *Struct. Bonding (Berlin)* **1991**, *76*, 51; f) P. Gütlich, A. Hauser, H. Spiering, *Angew. Chem. Int. Ed. Engl.* **1994**, *33*, 2024, and references cited therein; g) P. Gütlich, J. Jung, H. Goodwin, *Molecular Magnetism: From Molecular Assemblies to the Devices* (Ed.: Coronado et al.), NATO ASI Series E: Applied Sciences, **1996**, *321*, 327; h) P. Gütlich, H. A. Goodwin (Eds.), *Spin Crossover in Transition Metal Compounds I–III*, *Topics in Current Chemistry*, Springer-Verlag, Berlin, **2004**; i) J. A. Real, A. B. Gaspar, M. C. Munoz, *Dalton Trans.* **2005**, 2062; j) O. Sato, J. Tao, Y.-Z. Zhang, *Angew. Chem.* **2007**, *119*, 2200; *Angew. Chem. Int. Ed.* **2007**, *46*, 2152–2187.

[2] a) O. Kahn, C. Jay Martinez, *Science* **1998**, *279*, 44–48; b) O. Kahn, C. Jay, J. Kröber, R. Claude, F. Grolière, *Patent* **1995** EP0666561; c) J.-F. Létard, O. Nguyen, N. Daro, *Patent* **2005** FR0512476; d) J.-F. Létard, P. Guionneau, L. Goux-Capes, *Topics in Current Chemistry* (Eds.: P. Gütlich, H. A. Goodwin), Springer, NewYork, **2004**, *235*, 221.

[3] a) G. Psomas, N. Bréfuel, F. Dahan, J.-P. Tuchagues, *Inorg. Chem.* **2004**, *43*, 4590–4594; b) D. Boinnard, A. Bousseksou, A. Dworkin, J.-M. Savariault, F. Varret, J.-P. Tuchagues, *Inorg. Chem.* **1994**, *33*, 271–281; c) L. Salmon, A. Bousseksou, B. Donnadieu, J.-P. Tuchagues, *Inorg. Chem.* **2005**, *44*, 1763–1773.

[4] V. A. Grillo, L. R. Gahan, G. R. Hanson, R. Stranger, T. W. Hambley, K. S. Murray, B. Moubaraki, J. D. Cashion, *J. Chem. Soc., Dalton Trans.* **1998**, 2341–2348.

[5] J. S. Costa, C. Balde, C. Carbonera, D. Denux, A. Wattiaux, C. Desplanches, J. P. Ader, P. Gütlich, J.-F. Létard, *Inorg. Chem.* **2007**, *46*, 4114–4119.

[6] a) M. Nelson, P. D. A. Mcllroy, C. S. Stevenson, E. König, G. Ritter, J. Waigel, *J. Chem. Soc., Dalton Trans.* **1986**, 991; b) E. König, G. Ritter, J. Dengler, M. Nelson, *Inorg. Chem.* **1987**, *26*, 3582; c) S. Hayami, Z.-Z. Gu, Y. Einaga, Y. Kobayashi, Y. Ishikawa, Y. Yamada, A. Fujishima, O. Sato, *Inorg. Chem.* **2001**, *40*, 240; d) J. S. Costa, P. Guionneau, J.-F. Létard, *J. Phys.: Conference Ser.* **2005**, *21*, 67–72; e) P. Guionneau, F. Le Gac, A. Kaiba, J. S. Costa, J.-F. Létard, *Chem. Commun.* **2007**, 3723–3725.

[7] a) E.-G. Jäger, *Chemistry at the Beginning of the Third Millenium* (Eds.: L. Fabbrizzi, A. Poggi), Springer-Verlag, **2000**, 103–138; b) G. Leibeling, Ph. D. Thesis, Universiy of Jena, Germany, **2003**; c) B. R. Müller, G. Leibeling, E.-G. Jäger, *Chem. Phys. Lett.* **2000**, *319*, 368–374.

[8] B. Weber, E. Kaps, J. Weigand, C. Carbonera, J.-F. Létard, K. Achterhold, F.-G. Parak, *Inorg. Chem.* **2008**, *47*, 487–496.

[9] B. Weber, C. Carbonera, C. Desplances, J.-F. Létard, *Eur. J. Inorg. Chem.* **2008**, 1589–1598.

[10] L. Wolf, E.-G. Jäger, *Z. Anorg. Allg. Chem.* **1966**, *346*, 76.

[11] C. P. Slichter, H. G. Drickamer, *J. Chem. Phys.* **1972**, *56*, 2142–2160.

[12] K. F. Purcell, M. P. Edwards, *Inorg. Chem.* **1984**, *23*, 2620–2625.

[13] H. Spiering, E. Meissner, H. Köppen, E. W. Müller, P. Gütlich, *Chem. Phys.* **1982**, *68*, 65.

[14] B. Weber, R. Tandon, D. Himsl, *Z. Anorg. Allg. Chem.* **2007**, 1159–1162.

[15] B. Weber, E. S. Kaps, C. Desplanches, J.-F. Létard, *Eur. J. Inorg. Chem.* **2008**, 2963–2966.

[16] a) J. McGarvey, I. Lawthers, *J. Chem. Soc., Chem. Commun.* **1982**, 906; b) S. Decurtins, P. Gütlich, C. P. Köhler, H. Spiering, A. Hauser, *Chem. Phys. Lett.* **1984**, *105*, 1; c) S. Decurtins, P. Gütlich, K. M. Hasselbach, A. Hauser, H. Spiering, *Inorg. Chem.* **1985**, *24*, 2174; d) A. Hauser, *Chem. Phys. Lett.* **1986**, *124*, 543.

[17] A. Hauser, *Coord. Chem. Rev.* **1991**, *111*, 275.

[18] a) J. F. Létard, P. Guionneau, L. Rabardel, J. A. K. Howard, A. E. Goeta, D. Chasseau, O. Kahn, *Inorg. Chem.* **1998**, *37*, 4432–4441; b) J.-F. Létard, G. Chastanet, O. Nguyen, S. Marcen, M. Marchivie, P. Guionneau, D. Chasseau, P. Gütlich, *Monatsh. Chem.* **2003**, *134*, 165–182; c) J.-F. Létard, *J. Mater. Chem.* **2006**, *16*, 2550.

[19] a) J.-F. Létard, L. Capes, G. Chastanet, N. Moliner, S. Létard, J. A. Real, O. Kahn, *Chem. Phys. Lett.* **1999**, *313*, 115; b) S. Marcen, L. Lecren, L. Capes, H. A. Goodwin, J.-F. Létard, *Chem. Phys. Lett.* **2002**, *358*, 87; c) J.-F. Létard, P. Guionneau, O. Nguyen, J. S. Costa, S. Marcén, G. Chastanet, M. Marchivie, L. Capes, *Chem. Eur. J.* **2005**, *11*, 4582.

[20] *Organikum*, Johann Ambrosius Barth Verlagsgesellschaft mbH, Leipzig, Germany, **1993**.

[21] B. Heyn, B. Hipler, G. Kreisel, H. Schreer, D. Walter, *Anorganische Synthesechemie*, Springer-Verlag, Heidelberg, **1986**, 2nd ed..

[22] *X-RED 1.06*, Stoe & Cie, Darmstadt, Germany, **1996**.

[23] A. Altomare, M. C. Burla, G. M. Camalli, G. Cascarano, C. Giacovazzo, A. Guagliardi, A. G. G. Moliterni, G. Polidori, R. Spagna, *sir97*, Campus Universitario Bari, **1997**; A. Altomare, M. C. Burla, G. M. Camalli, G. Cascarano, C. Giacovazzo, A. Guagliardi, A. G. G. Moliterni, G. Polidori, R. Spagna, *J. Appl. Crystallogr.* **1999**, *32*, 115–119.

[24] G. M. Sheldrick, *shelxl 97*, University of Göttingen, Germany, **1993**.

[25] C. K. Johnson, M. N. Burnett, *ORTEP-III*, Oak-Ridge National Laboratory, Oak-Ridge, **1996**; L. J. Farrugia, *J. Appl. Crystallogr.* **1997**, *30*, 565.

Received: April 24, 2008
Published Online: September 16, 2008

